



Sonochemical recovery of uranium from nanosilica-based sorbent and its biohybrid

S. Lahiri^{a,d,*}, A. Mishra^b, D. Mandal^{c,d}, R.L. Bhardwaj^a, P.R. Gogate^e

^a Laser & Plasma Technology Division, Bhabha Atomic Research Centre, Mumbai 400085, India

^b Nuclear Agriculture & Biotechnology Division, Bhabha Atomic Research Centre, Mumbai 400085, India

^c Alkali Material & Metal Division, Bhabha Atomic Research Centre, Mumbai 400085, India

^d Homi Bhabha National Institute, Anushaktinagar, Trombay, Mumbai 400094, India

^e Chemical Engineering Department, Institute of Chemical Technology, Matunga, Mumbai 400019, India

ARTICLE INFO

Keywords:

Uranium recovery
Ultrasound
Intensification
Silica nanoparticles
Biohybrid

ABSTRACT

Use of nanomaterials to remove uranium by adsorption from nuclear wastewater is widely applied, though not much work is focused on the recovery of uranium from the sorbents. The present work reports the recovery of adsorbed uranium from the microstructures of silica nanoparticles (SiO₂M) and its functionalized biohybrid (^fBHM), synthesized with *Streptococcus lactis* cells and SiO₂M, intensified using ultrasound. Effects of temperature, concentration of leachant (nitric acid), sonic intensity, and operating frequency on the recovery as well as kinetics of recovery were thoroughly studied. A comparison with the silent operation demonstrated five and two fold increase due to the use of ultrasound under optimum conditions in the dissolution from SiO₂M and ^fBHM respectively. Results of the subsequent adsorption studies using both the sorbents after sonochemical desorption have also been presented with an aim of checking the efficacy of reusing the adsorbent back in wastewater treatment. The SiO₂M and ^fBHM adsorbed 69% and 67% of uranium respectively in the second cycle. The adsorption capacity of ^fBHM was found to reduce from 92% in the first cycle to 67% due to loss of adsorption sites in the acid treatment. Recovery and reuse of both the nuclear material and the sorbent (with some make up or activation) would ensure an effective nuclear remediation technique, catering to UN's Sustainable Development Goals.

1. Introduction

Uranium is the most common radionuclide used as fuel in the nuclear power industry and hence it also constitutes the highest proportion in the nuclear wastewater, posing environmental hazard [1–3]. Due to limited reserves of uranium in India, its recovery from unconventional uranium sources viz. wastewater from uranium mines (containing 480–560 ppm of uranium) [4], fertilizer industry (viz. uranium bearing phosphate as raw material) [5,6] and nuclear reprocessing facilities, mill tailings [4], rock phosphate [6,7] or even seawater (having 3 ppb of uranium) [8] is of particular interest. Efforts are being made to recover the uranium from such lean sources to conserve the natural reserves and also to minimize the spread of contamination of nuclear materials in the environment [9]. Chemical precipitation, solvent extraction, cementation, electrochemical oxidation, evaporation and adsorption are a few of the conventional methods used for the removal of uranium from

aqueous solution [10–13]. Most of these methods also have some drawbacks such as uneconomical operation, generation of toxic wastes, low efficiency and high energy consumption [12]. Specifically, adsorption is the most efficient and simplest process for removing contaminants from wastewater [11,13,14] though it also generates secondary waste in the form of used sorbents, which is a very significant aspect in nuclear wastewater treatment. If proper methods are developed for efficient recovery from the sorbents, its subsequent reuse in the fuel cycle is possible and in addition sorbent can also be reused. Recycle of uranium will prevent waste of valuable fissile material resource and also reduce the associated environmental concerns.

Recent developments in nanotechnology have paved a way for the use of nanomaterials such as silica nanoparticles [13], graphene oxide [14], titanium oxide [15], carbon nanotubes [16], nanozeolite composites [17], magnetic nanoparticles [18] and nanoalumina [19,20] as effective sorbents. Silica based matrices has gained a lot of interest as

* Corresponding author at: Laser & Plasma Technology Division, Bhabha Atomic Research Centre, Mumbai 400085, India.

E-mail address: sutanwi@barc.gov.in (S. Lahiri).

<https://doi.org/10.1016/j.ultsonch.2021.105667>

Received 1 June 2021; Received in revised form 2 July 2021; Accepted 5 July 2021

Available online 8 July 2021

1350-4177/© 2021 The Author(s).

Published by Elsevier B.V. This is an open access article under the CC BY-NC-ND license

(<http://creativecommons.org/licenses/by-nc-nd/4.0/>).

sorbent due to their characteristic features [21–23]. Silica, in the form of non-functionalized nanoparticles [24–27] as well as functionalized mesoporous particles [27–30] has been widely used for sorption of uranium ions because of high reactivity and environmental mobility. For example, Functionalized silica based supports using *Streptococcus lactis* cells as functionalizing agent, synthesized using spray drying demonstrated good sorption characteristics, as reported earlier [29]. The bio-hybrid showed almost the same adsorption capacity ($92 \pm 2\%$) as that of activated carbon ($92 \pm 4\%$) [30]. However, these sorbents form secondary radioactive wastes, and pose a burden to the nuclear reprocessing facilities. The recovery of uranium from the synthesized biohybrid as well as spray dried silica microstructures is also important to reuse uranium in the nuclear fuel cycle. The recovery aspect of metals from the sorbents has not yet been explored.

The novelty of the present work lies in the demonstration of an efficient sonochemical process for the recovery of uranium from the nanosilica based microstructures. Sonochemical leaching is a widely used efficient process for recovery of adsorbents as also demonstrated for graphite substrate [24]. The most pertinent effects of ultrasound in liquid–solid systems are mechanical effects. When a cavitation bubble collapses, microjets of the solvent impinging on the surface lead to cleaning or dislodging of adsorbed metal. An increase in the resultant microstreaming further increases the mass transfer across the boundary layer as well as possibly thinning of the film and effective desorption is obtained as also reported for nuclear materials [32–39].

In the present work, parametric studies and leaching kinetics of uranium from the ^fBHM bio-hybrid (comprising bacterial cells and silica nanoparticles) as well as from spray dried silica microstructures (SiO_2M) were studied. Biological components like bacterial cells are highly sensitive against various chemicals and are mechanically less stable [29]. Thus, this study helps to understand the changes/transformations happening in physical as well as chemical properties of ^fBHM and SiO_2M during the process of sonochemical leaching of uranium. The work also opens a new dimension in nuclear remediation technique wherein recovery of nuclear materials of interest from bio-hybrids could be achieved, allowing its recycle in the fuel cycle and preventing the generation of secondary wastes. The study further demonstrates the reusability of both the adsorbents (SiO_2M and ^fBHM) after sonication induced recovery. Though recovery of uranium from activated carbon can be achieved easily by burning off the sorbent, it would cause environment pollution and sorbent recyclability is not be possible demonstrating the importance of the approach presented in current work.

2. Materials and methods

2.1. Materials

Colloidal silica nanoparticle suspension (40 v/v%) was purchased from Visa Chemicals, India. The colloidal solution contains 40 wt% silica, having a specific surface area of $220 \text{ m}^2/\text{g}$ and density as 1.3 g/ml at 25°C , as specified by the manufacturer. The particle size varied between 12 nm and 17 nm. A stock solution of uranium (500 ppm) was prepared using $\text{UO}_2(\text{NO}_3)_2 \cdot 6\text{H}_2\text{O}$ (Merck, Germany) in double-distilled water. *S. lactis* cells were overnight grown in MRS Broth and used for further studies. A high concentration of uranium would ensure that the binding sites on the sorbent are saturated with the metal ion, as also reported by Mishra et al. [29]. The concentration of uranium in the mine wastewater is also in the same range confirming the selection of concentration as 500 ppm. Nitric acid ($\sim 16 \text{ M}$) was obtained from M/s Sigma Aldrich. All chemicals were of analytical grade.

2.2. Synthesis of SiO_2 microstructures (SiO_2M) and bio-hybrid microstructures (^fBHM)

For the synthesis of spray dried SiO_2 microstructures, 100 mL of silica NP (2 v/v%) solution was prepared and used as feed through the

nozzle of spray dryer (LU222, Labultima, India) maintained under a flow of hot air at inlet temperature (140°C) and flow rate 2 mL min^{-1} . After spray drying, fine dried powder was recovered at 55°C as the outlet temperature. The spray dried powder was stored at 4°C and used for further studies.

In the case of ^fBHM , overnight grown *S. lactis* cells (6 w/v%) were mixed in silica NP (2 v/v%) solution, stirred for 30 min and used as feed for spray dryer operated as mentioned above. The spray dried powder was stored at 4°C and used for further studies. The details of the synthesis of both SiO_2M and ^fBHM are reported in details, in our earlier publication [29].

2.3. Synthesis of uranium loaded SiO_2 microstructures (SiO_2M) and bio-hybrid microstructures (^fBHM)

For the synthesis of uranium loaded SiO_2M and ^fBHM , SiO_2M (1 g L^{-1}) and ^fBHM (1 g L^{-1}) was mixed separately in uranium solution (100 mg L^{-1}), and agitated on the shaker (MaxQ 4000, Thermo, USA) working at room temperature (298 K) at 100 rpm for 2 h. Solution was centrifuged at 9000 rpm for 5 min (Eppendorf centrifuge, Model-5810R, Germany). The supernatant was used to analyze residual uranium concentration and pellet (uranium loaded SiO_2M and uranium loaded ^fBHM) was stored till further use.

2.4. Leach solutions and experimental setup for dissolution

The resultant uranium adsorbed sorbents (SiO_2M and ^fBHM) were treated with different concentrations of nitric acid (HNO_3) and ultrasonic baths of different frequencies (20 ± 2 , 30 ± 3 and $40 \pm 3 \text{ kHz}$) have been used. The in-house built ultrasonic cleaning bath has dimensions of height, width and depth as $240 \text{ mm} \times 140 \text{ mm} \times 60 \text{ mm}$, respectively (Fig. 1). Two transducers (M/s Morgan Matrac make) of size 2" each operating at the same frequency were attached to the base of the tank.

Uranium loaded sorbents (SiO_2M and ^fBHM) taken in a beaker with 10 mL of 4 M HNO_3 solution were mounted on a metal basket and dipped in the bath. The acoustic intensity was maintained at 8 W cm^{-2} (80 W) in all experiments, except in cases where the effect of ultrasonic intensity was studied. The power dissipation was varied between 20 and 100 W to study the effect of intensity, in order to achieve the requisite acoustic intensity. The ultrasonic bath was filled with distilled water upto a level of 30 mm to provide a medium for sonication. The bath was placed in a fumehood to manage the NOx fumes generated where suitable dilution was provided with air. Dissolution studies were carried out in batches for 30 min each (unless otherwise mentioned). All the experiments were carried out in triplicate, and the mean values have been reported with experimental errors typically between $\pm 3\%$.

2.5. Analysis of leach liquor samples

The leach liquor samples were withdrawn at equal intervals of time, filtered and analyzed for dissolved uranium concentration. Estimation of uranium was performed using inductively-coupled plasma optical

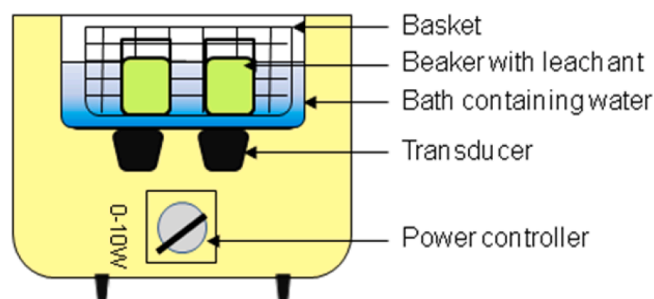


Fig. 1. Experimental setup.

emission spectroscopy (ICPOES). In each set, uranium solution (without sorbent) was used as control.

2.6. Characterization of morphology

To study the changes in morphology of the sorbents (SiO_2M and f^{BHM}) before and after desorption of uranium, Scanning Electron Microscopy (SEM) (Make: M/s Tescan Vega3) analysis was carried out. Energy Dispersive Spectroscopy (EDS) studies were also carried out in parallel using detector from M/s Oxford Instruments. To understand the involvement of functional groups of sorbents, Fourier transform infrared spectroscopy (FTIR) of the sorbents was recorded using Bruker FT-IR Alpha II spectrometer, at a resolution of 4 cm^{-1} . Raman spectrometer (M/s WITec make, Model Alpha 300R) was used to make a comparative study of the uranyl compounds present in the biohybrid before and after sonication.

2.7. Reusability studies after sonication

In order to test the reusability of the nanoparticles, 1 g L^{-1} of sorbent and uranyl nitrate solution of 50 mg L^{-1} concentration (initial pH = 7.0) was agitated on a rotary shaker operating at room temperature (298 K) and 150 rpm for 24 h. The objective was to measure the uranium adsorption capacity on reuse for adsorption.

3. Results and discussion

3.1. Recovery of uranium using only acid (in the absence of ultrasonic field)

The obtained results for recovery of uranium from both SiO_2M and f^{BHM} are shown in Fig. 2 (a) and Fig. 2 (b) respectively. Nitric acid is widely used for uranium recovery [39]. The extent of dissolution of uranium with 8 M nitric acid at the operating temperature $45\text{ }^\circ\text{C}$ was less than 6% and 20% in 1 h for both SiO_2M and f^{BHM} respectively in the absence of ultrasonic field. The concentration of the acid was deliberately taken as 8 M to allow considerable recovery of metal from the microstructures, though results were not very promising in the absence of ultrasound. In addition, Despite the higher adsorption capacity of the f^{BHM} compared to the SiO_2M , as reported earlier [23], the recovery of uranium from the f^{BHM} was faster than SiO_2M .

The effect of concentration of the acid on the biohybrid on uranium recovery was studied through Scanning Electron Microscopy (SEM) analysis. In Fig. 3 (a-d), micrographs show the trends for degradation of the biohybrid at different acid concentration at room temperature in the absence of ultrasound. Higher recovery of uranium from the biohybrid compared to the self assembled SiO_2M can be explained by the micrographs (Fig. 3 (b)) which show the disintegration of the f^{BHM} in acid beyond 4 M acid concentration. At 4 M acid concentration, fissures appear on the surface and beyond 4 M concentration, the biohybrid collapses to a deformed two-dimensional structure (Fig. 3 (c)) from its three-dimensional dough-nut shaped morphology. The biohybrid shows complete disintegration at 16 M acid (Fig. 3 (d)). Similar results were observed in the presence of ultrasound (20 kHz and 40 kHz) thereby establishing acid concentration as the sole reason for the degradation of biohybrid and not ultrasonic cavitation. On sonicating the solution in water, degradation of the cells was not observed. This observation has also been confirmed by earlier reports [40–44] that state that cell lysis is brought about by ultrasound only at very high intensity ($>10\text{ W/cm}^2$).

Though the effect of ultrasound on bacterial cells is limited, lysis of tumor cells is reported say using focused ultrasound [45]. However, effect of nitric oxide on cell disintegration is widely reported [46]. Therefore, it may be concluded that at higher nitric acid concentration, the nitric oxide generation leads to the disintegration of the cells more dominantly as compared to ultrasound.

The particle size distribution of the biohybrid in various acid

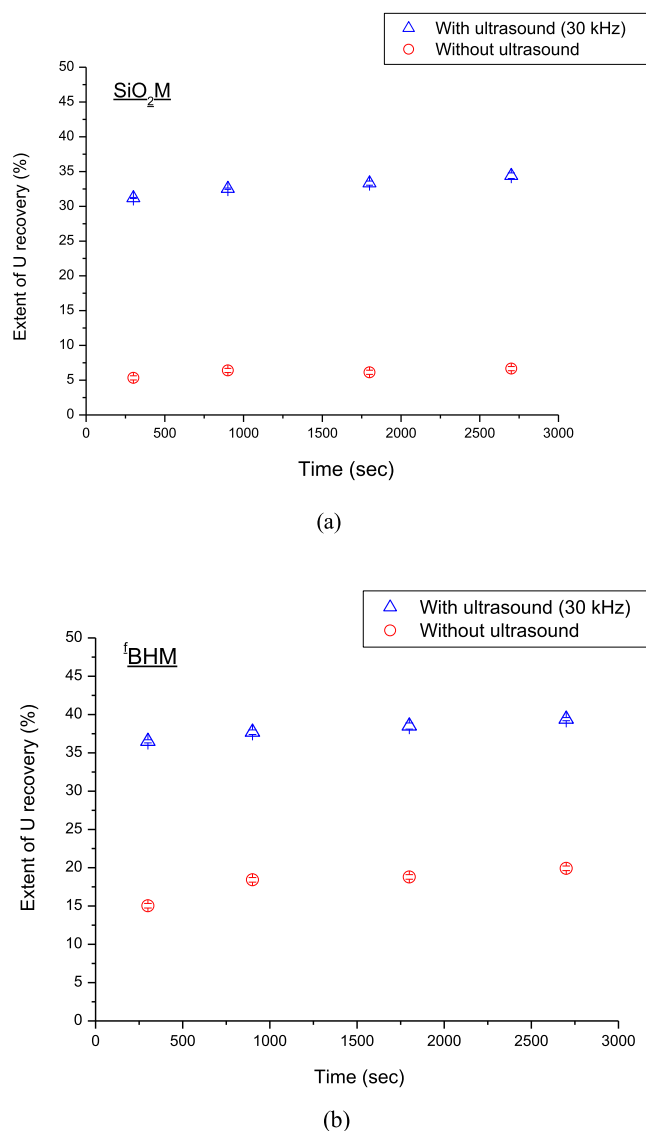


Fig. 2. Comparison of uranium recovery with and without ultrasound for (a) SiO_2M (b) f^{BHM} .

concentrations corroborates the initiation of degradation of the microstructures beyond 4 M acid (Fig. 3 (e)). The particle size of the biohybrid remains intact till 4 M, beyond which it gets skewed towards size $<1\text{ }\mu\text{m}$. Around 7% of the total particle volume is less than $1\text{ }\mu\text{m}$ when treated with 8 M acid and 55% becomes lower in the case of acid of 16 M concentration as depicted schematically in Fig. 4.

Thermal effect on biohybrid was also studied in the absence of ultrasound to confirm degradation of biohybrid microstructure beyond $70\text{ }^\circ\text{C}$. The degradation of biohybrid was observed to some extent at $70\text{ }^\circ\text{C}$ (Fig. 5 (a)), but complete disintegration is seen beyond $100\text{ }^\circ\text{C}$ (Fig. 5 (b)) which is attributed to the combined effect of acid and temperature on the cells. Therefore, high acid concentration and high temperature intensification of uranium recovery is ruled out for the biohybrid.

3.2. Intensification of recovery using ultrasound

The poor recovery rates of uranium from SiO_2M and f^{BHM} microstructures necessitated the use of sonochemical intensification. Ultrasound is an interesting alternative for low temperature ($<70\text{ }^\circ\text{C}$) process intensification. Since the piezoelectric transducers used to generate

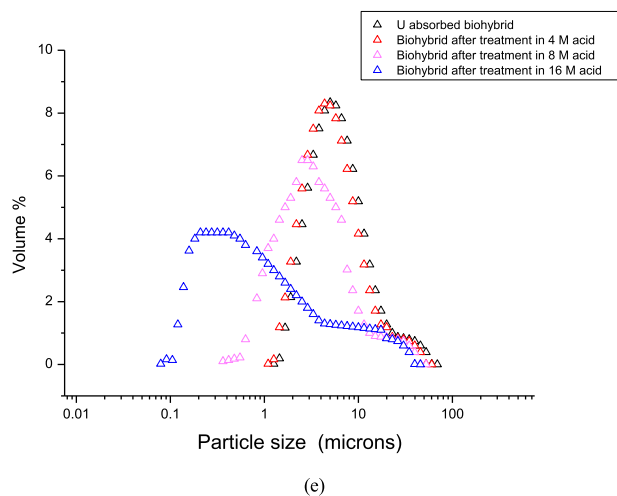
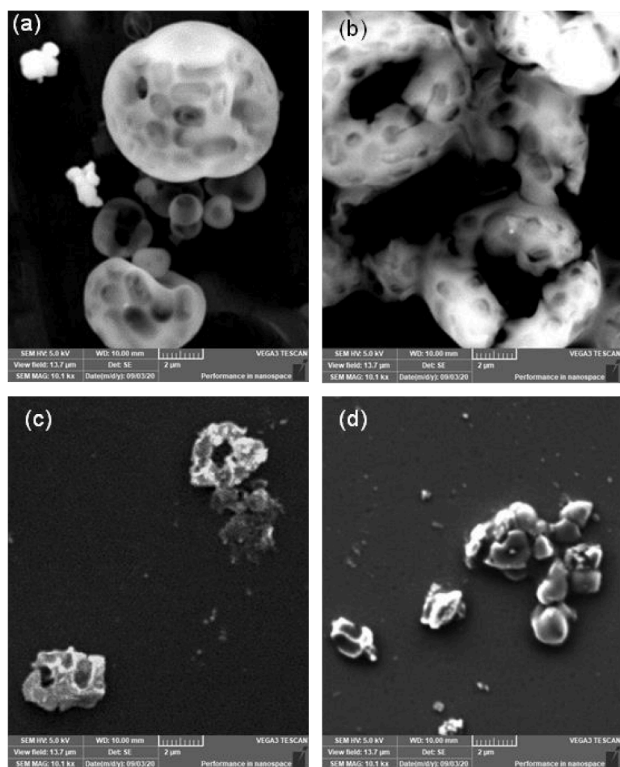


Fig. 3. Silica biohybrid after treatment in nitric acid (30 °C for 30 min) of varying concentration SEM images (a) 1 M, (b) 4 M, (c) 8 M and (d) 16 M; (e) particle size distribution after treatment in different acid concentration.

ultrasonic field has a curie temperature of 120 °C, the bath temperature is also kept sufficiently low to prevent damage to the piezoelectric crystal (Lead Zirconate Titanate, PZT, in our case) and the glue bonding the transducer to the reactor bottom. Ultrasound has been demonstrated to successfully increase mass transfer rates, improve yields, and initiate reactions and even change the reaction pathways [34,36,37]. In order to establish the intensification effects of ultrasound in the dissolution and recovery process of uranium from the microstructures, the extent of dissolution at 30 kHz ultrasonic field under similar operating conditions was studied. It is clearly established from Fig. 2 (a) for SiO₂M and Fig. 2 (b) for ^fBHM that the ultrasonic dissolution yields five- and two-fold enhancement in the extent of dissolution, respectively. The intensification is caused by the cavitating bubbles that act as microreactors of high temperature and pressure, resulting in faster dissolution of uranium in

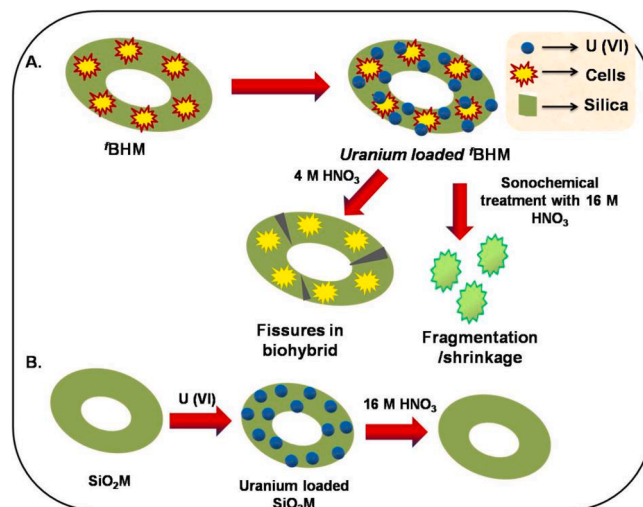


Fig. 4. Schematic showing desorption of U from (A) ^fBHM and (B) SiO₂M.

the acid before their collapse on the surface of the silica substrates. The impact of collapse of bubbles further leads to dislodging of the contaminants from the surface facilitating enhanced recovery.

The micrographs of the SiO₂M and ^fBHM before adsorption of the metal, after adsorption and after recovery of metal by sonication have been given in Fig. 6. Fig. 6 (a) shows the microstructure of the silica (SiO₂M) before adsorption. The SiO₂M after adsorption of uranium is represented in Fig. 6 (b). Fig. 6 (c) shows SiO₂M after desorption using 30 kHz ultrasonic field applied at 16 M acid concentration for 30 min. As evident from the micrographs, the SiO₂M shows no difference in morphology before and after recovery of uranium. The results clearly confirm that the morphology remains unaffected by the temperature, high acid molarity and the effect of the cavitating bubbles leaching out the adsorbed U from its surface.

On the other hand, the ^fBHM presents a contrasting picture based on the comparison of the native material, after adsorption and finally after desorption based on ultrasound. The morphology of the doughnut shaped self-assembled spray dried structure shows the prominence of cells near the surface in the case of native adsorbent (Fig. 6 (d)). The doughnut shaped structure can be explained by the repulsion of the negatively charged silanol groups on silica and the negatively charged cell wall of the cells, as discussed elsewhere [29]. These cells on the surface gets occupied with uranium due to the adsorption and the prominent imprints of the cells are less visible (Fig. 6 (e)). After sonication treatment using 16 M acid leading to uranium recovery, the biohybrid doughnut structure collapse to a deformed structure (Fig. 6 (f)). This was mainly due to the high acid concentration and not due to ultrasound effects as also discussed earlier and confirmed by dissolving the biohybrid in 16 M acid in the absence of any ultrasonic field. The acid degraded the cells and the three dimensional doughnut structure collapsed, subsequently fragmenting into smaller particles, even in the absence of ultrasound. Therefore, detrimental effect of high acid concentration on the biohybrid is conclusively proved, also confirming that use of ultrasound is not contributing to any negative effects.

Raman spectra of the uranium adsorbed biohybrid before sonication and after sonication using 4 M acid for 30 min are shown in Fig. 7 (a). The uranyl (UO₂²⁺) peaks in the spectra (at 177 and 845 cm⁻¹) before sonication reduce in intensity after sonication, indicating leaching of the metal ions from the substrate. The peaks at 745, 1046 and 1400 cm⁻¹ are known to be nitrate vibrational modes [47].

The EDS study of the biohybrid before sonication and after sonication using 4 M acid for 30 min is shown in Fig. 7 (b). The study demonstrated a reduction of U content in the biohybrid from 21% (w/w) to 3% (w/w) after 30 min of sonication.

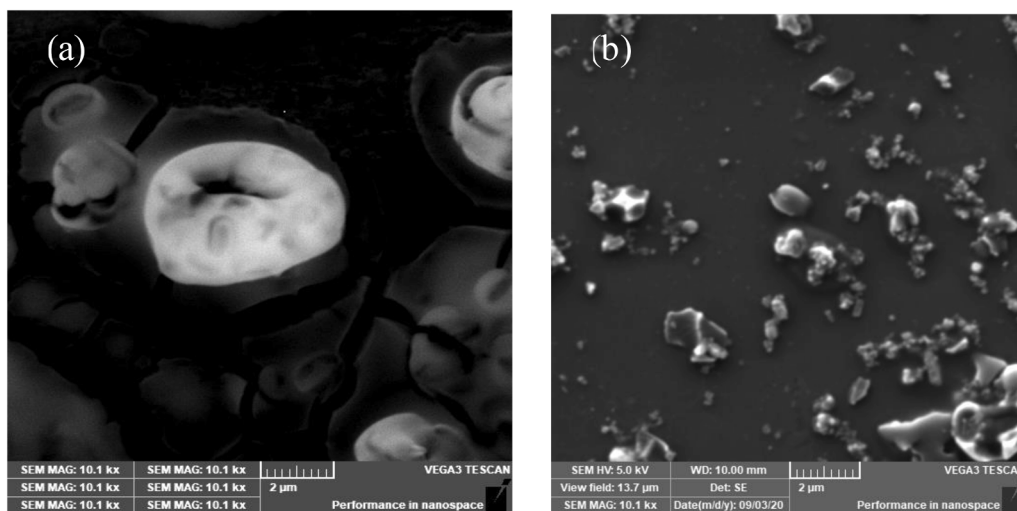


Fig. 5. β BHM after treatment in nitric acid (1 M, 30 min) at (a) 70 °C, (b) 100 °C.

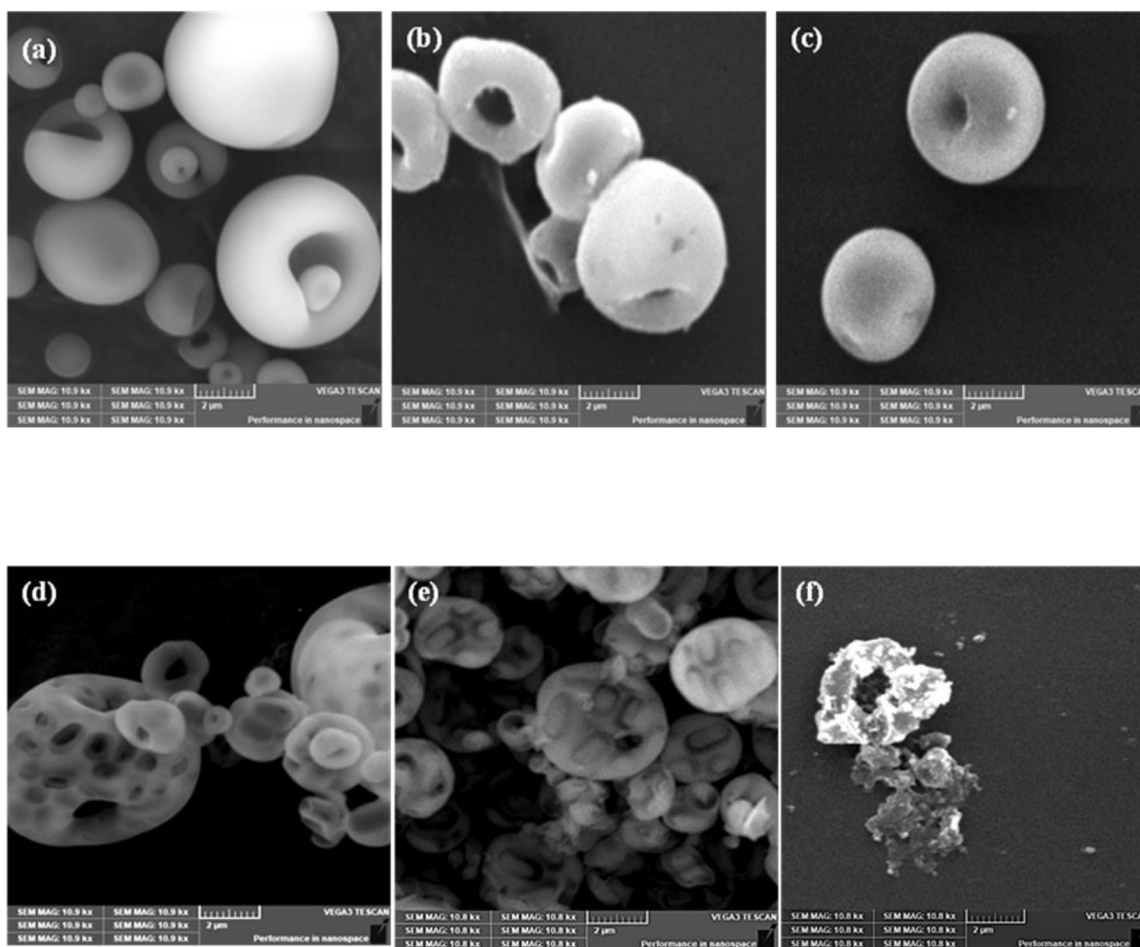
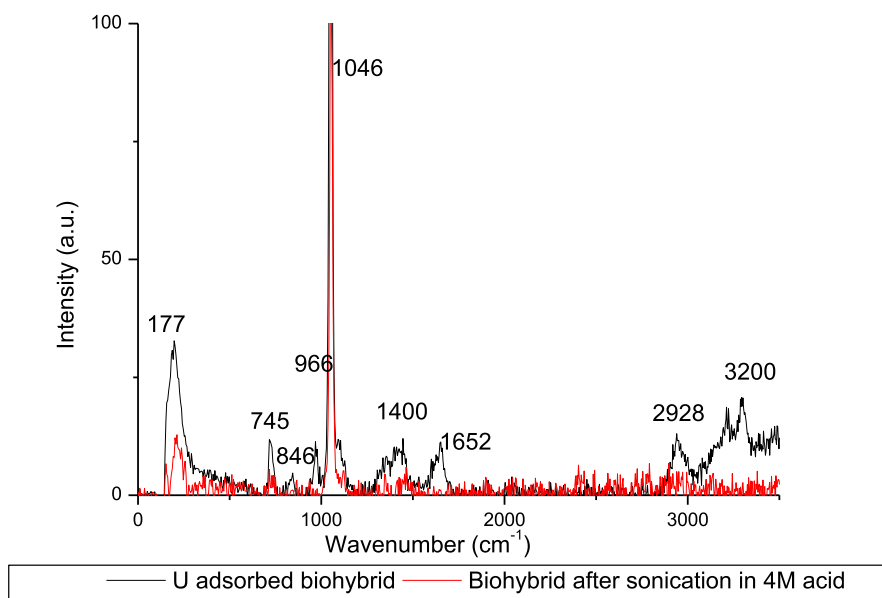


Fig. 6. SEM Micrographs of spray dried silica microparticles (SiO_2M) (a) before and (b) after adsorption of uranium, (c) SiO_2M after leaching out uranium at 30 kHz using 16 M acid for 30 min, (d) β BHM before adsorption and (e) after adsorption of metal, (f) β BHM after sonication treatment using 8 M acid for 30 min.

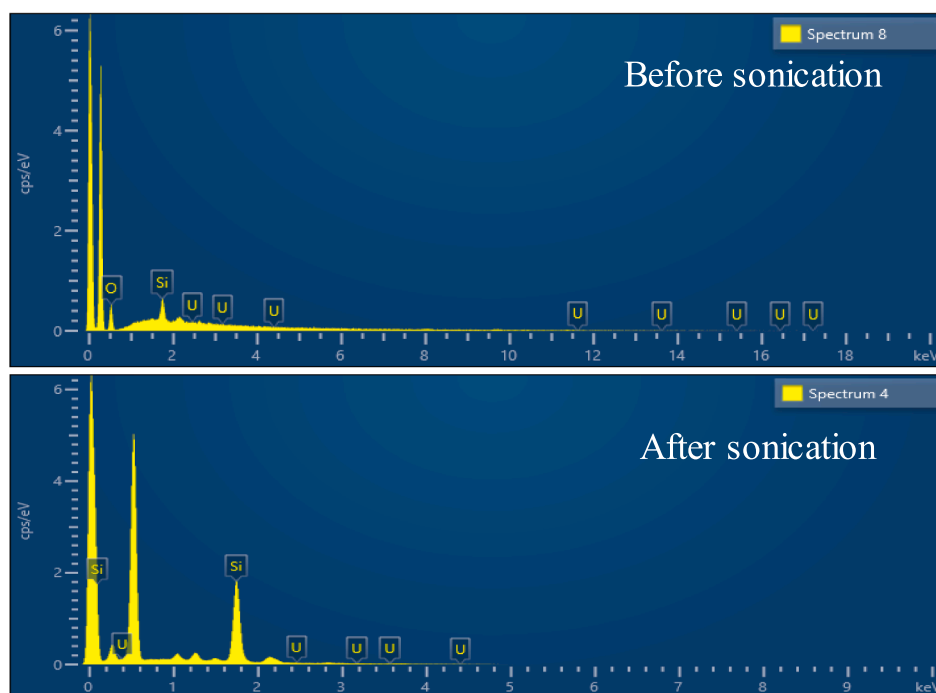
In order to study the effect of operating parameters in the intensified dissolution, the effect of acid concentration, temperature, operating frequency and acoustic intensity were subsequently studied and now discussed.

3.3. Effect of acid concentration on intensified dissolution

The plots given in the Fig. 8 (a) explains the dependence of the dissolution ratios with time at different concentrations of HNO_3 . Nitric acid is a strong oxidizing agent that oxidizes the U(IV) to U(VI) and it is expected that the rate of oxidation will be dependent on the



(a)



(b)

Fig. 7. Comparison of (a) Raman Spectra and (b) EDS study before sonication and after sonication using 4 M acid for 30 min.

concentration. With 2 M HNO_3 , minimal extents of dissolution were seen for both SiO_2M and ^1BHM which increased almost linearly with the loading of HNO_3 at the same temperature of 45 °C for a sonication time of 30 min. As the acid concentration increases, metal recovery from SiO_2M shows a linear increase due to faster dissolution in acid. Comparatively, ^1BHM shows a gradual rise till 12 M acid, beyond which the U recovery increases dominantly which may be attributed to breakdown of the cellular composition in high acid concentration and

faster release of the adsorbed uranium into the solution. The same was confirmed by the disintegration and collapse of the doughnut shaped structure as demonstrated in Fig. 2 (f) for the case of 16 M acid strength. Even in the case of U recovery from graphite, too high acid strength was observed to lead to pitting corrosion of the substrate [32,39]. Therefore, though the leaching of uranium from SiO_2M would be fastest in 16 M acid but due to the damage to the structure of SiO_2M , high release of NO_x gases from the dissolution process and stringent requirement on the

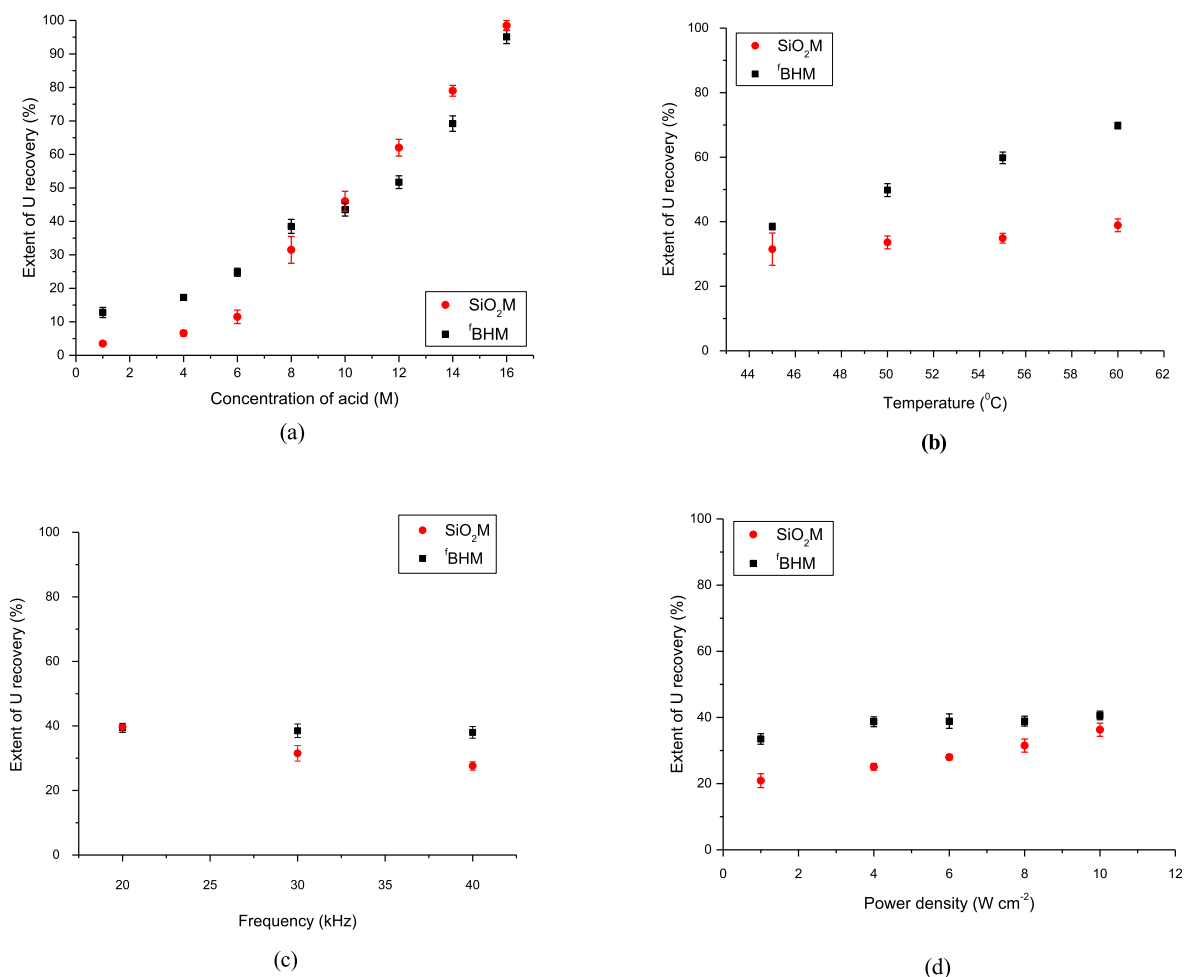


Fig. 8. (a) Effect of concentration of acid on uranium recovery (30 kHz, 8 W cm⁻² acoustic intensity) (b) Effect of temperature of acid on uranium recovery (30 kHz, 8 W cm⁻² acoustic intensity) (c) Effect of operating frequency on uranium recovery (at 45 °C, 8 M acid, 8 W cm⁻² acoustic intensity) (d) Effect of acoustic intensity on uranium recovery (at 45 °C, 8 M acid, 30 kHz).

material of construction for the ultrasonic bath, very high concentration of acid is considered to be difficult to handle on a large scale. Though a lower acid concentration is always beneficial, it sacrifices the rate and extent of recovery. At 45 °C and 20 kHz acoustic field, the recovery of uranium is 10% at 2 M and 17% at 4 M acid concentration. Therefore, 4 M acid was recommended for uranium recovery for both SiO₂M and fBHM.

3.4. Effect of temperature on intensified dissolution

The experiments to study the effect of temperature were carried out using different operating temperatures selected over the range of 40 °C to 60 °C using 4 M HNO₃ solution under 30 ± 3 kHz ultrasonic field with an acoustic intensity of 8 W cm⁻² (80 W power) applied for 30 min. The results for the effect of temperature on the dissolution of uranium are illustrated in Fig. 8 (b). The experimental results showed that while the temperature of the acid leachant had little effect (a change of less than 5% over the experimental range) on the silica nanoparticles, the dissolution from the fBHM was a more kinetically controlled process. Quantitatively, the extent of dissolution from SiO₂M only increased from 31% to 39% whereas dissolution from fBHM increased from about 40% to more than 60% with an increase in temperature from 40 °C to 60 °C for the case of 8 M HNO₃ (as seen in Fig. 8 (b)). An increase in the temperature usually increases the kinetic rate of dissolution which is evident in the present case. The ease of generation of cavities also increases due to the increase in the vapour pressure of the solution, also leading to

faster dissolution at 8 W cm⁻² [36,37]. The dampening of the overall sonication effect at higher temperatures due to cushioning effect of the bubbles is not observed in the present study giving a continuous increase in the dissolution rate with an increase in the temperature over the investigated range. Further, the leaching of SiO₂M was less sensitive to the temperature changes compared to fBHM. This may be explained by the fact that though silica remains unaffected in the studied temperature range, the temperature sensitive constituents (especially proteins) of the cells are affected by the temperature of the leachant. Therefore, the cells lose their binding capacity and release the adsorbed metal faster compared to SiO₂M. Considering the observed results, the recommended temperature for both SiO₂M and fBHM would be 60 °C in terms of faster dissolution or 45 °C in terms of better recovery of sorbent. In this work, the studies were carried out at the lowest temperature 45 °C to prevent masking of the effects of other parameters by the thermal effects. It is interesting to note that the effect of temperature on the dissolution from microstructures was similar to the trend observed in case of uranium recovery from the pores of graphite [24].

3.5. Effect of operating frequency of ultrasound

The available transducers of frequencies as 20 kHz, 30 kHz and 40 kHz (in the low frequency range) were used to characterize the effect of frequency on uranium recovery. The acoustic intensity maintained for all the operating frequency was fixed at 8 W cm⁻² (80 W as the actual supplied power). The dissolution tests for different frequencies were

conducted using 8 M acid at 40 °C. It was observed that the recovery of uranium from SiO₂M decreases with an increase in the operating frequency. The recovery was 40% at 20 kHz as the frequency, 30% at 30 kHz as the frequency and 26% at 40 kHz frequency (Fig. 8 (c)). At lower frequencies, the bubbles formed are larger, collapse violently and hence they render higher intensity mechanical effect on the substrate to dislodge the contaminants. The strong cavitation effect assisting the reaction with the acid dislodges the uranium from the surface of SiO₂M at a faster rate. Based on the obtained results, the recommended operating frequency for SiO₂M is 20 kHz. Similar trend was also reported for the case of uranium and yttria recovery from graphite substrate [32,39].

In the case of ^fBHM, the recovery showed hardly any change within the tested frequency range. The recovery of uranium from ^fBHM is more sensitive to chemical effects than mechanical effects of ultrasound. Therefore, no significant change was observed over the narrow range of frequency tested.

3.6. Effect of acoustic intensity

The acoustic intensity must exceed a certain threshold intensity to induce cavitation at desirable intensity and bring out the desired intensification. The obtained data for effect of acoustic intensity on the recovery in the case of SiO₂M and ^fBHM is shown in Fig. 8 (d). It is clearly established that the metal recovery from SiO₂M increases linearly with an increase in the applied acoustic intensity. The intensification in the reaction rate is a strong function of input power as increase in acoustic intensity increases the cavitation bubble density. These bubbles act as microreactors of high temperature and pressure and accelerate the dissolution process. Increase in acoustic intensity also increases the mechanical effect of ultrasound, as bubbles formation and subsequent implosion increases in turn accelerating the dissolution process.

It was also observed that the metal recovery from the ^fBHM is faster giving higher extent of recovery compared to that obtained in the case of SiO₂M. It is also important to note that at much higher vibrational amplitude, a large number of bubbles are generated which build up near the source of ultrasound and act as barrier in the transfer of acoustic energy to the liquid. This phenomenon is called source decoupling leading to a lowering of the effect of cavitation. The trend was clearly seen for the case of ^fBHM where the recovery was seen saturating beyond 5 W cm⁻² for an operating frequency of 20 kHz in the tested intensity range. Beyond the acoustic intensity of 5 W cm⁻² not much difference in the extent of recovery is seen. Interestingly, no such decoupling or cushioning effects were observed for SiO₂M over the range of power intensity investigated in the current work. Lower extents of recovery in the case of SiO₂M can be one of the reasons for the observed continuous increase in the extent of dissolution meaning that there is still some way to go before saturation is seen. In the case of recovery of uranium from graphite pores [31], the extent of dissolution also reached a peak indicating that the trends are dependent on the specific substrate materials making the study presented in the current work important.

3.7. Recyclability of the silica substrates after sonication

As discussed in section 3.2, the SiO₂M retains its original shape and size after sonication and appears to be less affected by the combined action of cavitation and acid compared to its biohybrid. Considering this analysis, SiO₂M was used for adsorption studies after ultrasound assisted leaching just to confirm the reusability. It was found that the SiO₂M adsorbs 69 ± 7% of uranyl nitrate solution after 24 h of agitation. The FTIR spectrum of the SiO₂M after U adsorption confirms the presence of Si-O-Si bond at ~ 1090 cm⁻¹ and Si-OH bond at 900 cm⁻¹ (Fig. 9 (a)). The broad centered peak at 3200 to 3500 cm⁻¹ was assigned to OH stretch. The peak around 600–800 cm⁻¹ may be attributed to the presence of UO_x. Thus it can be clearly said that SiO₂M is effectively reused for uranium adsorption.

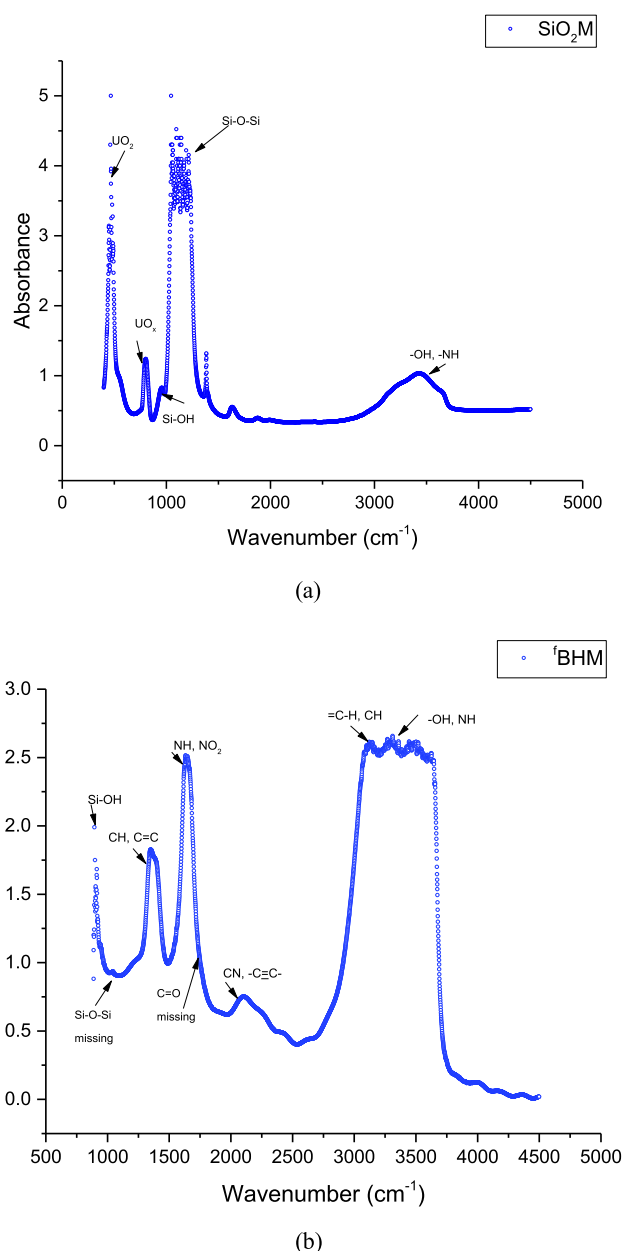


Fig. 9. FTIR spectra of (a) SiO₂M and (b) ^fBHM after adsorption of uranium.

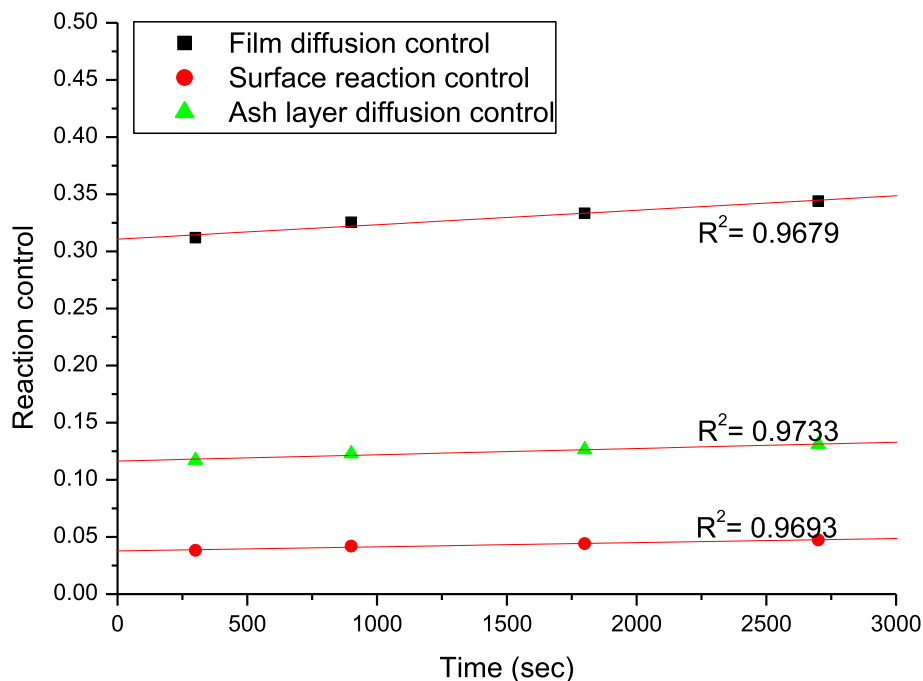
Reusability studies on biohybrid treated with 1 M acid was found to yield removal of 60 ± 3% of the uranyl nitrate mother liquor, while biohybrid sonicated in 4 M acid adsorbs 58 ± 2%. These values are less than 92 ± 2% uranium uptake, earlier reported [29] which may be attributed to the loss of adsorption sites due to the acid treatment.

The reusability studies on biohybrid treated beyond 4 M acid were not repeatable. The FTIR study of the ^fBHM before sonication treatment has been reported by Mishra *et al.* [29]. Comparing the FTIR spectra of ^fBHM after sonication in 20 kHz ultrasonic field (Fig. 9 (b)) using 16 M acid (without adsorbing U) with that before sonication, we find that the Si-O-Si group (~1090 cm⁻¹) and the C = O group (~1700 cm⁻¹) are missing after treatment. The only detectable silica signature was at 900 cm⁻¹ as the asymmetric vibration of Si-OH. This change may be attributed to the reaction of acid and silanol groups after the breakdown of the biohybrid. The -CH and C = C stretch at ~ 1400 cm⁻¹, -NH and NO₂ stretch at ~ 1550 cm⁻¹, =C-H, -CH around 3100 cm⁻¹, and -OH and -NH stretch at ~ 3200–3500 cm⁻¹ (due to water and trapped acid) are the few other dominant peaks observed. It can be concluded that due

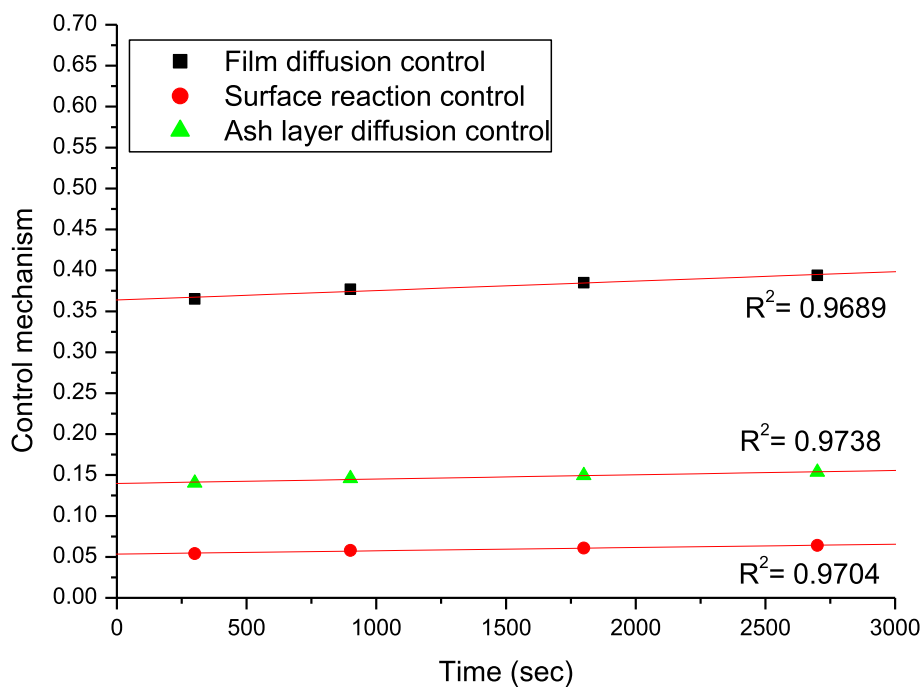
to the structural deformation and disintegration of the f BHM mainly in high acid concentration, the major adsorption sites like Si-O-Si, C = O, were missing. Therefore, the reusability studies on the recycled f BHM beyond 4 M acid concentration were not repeatable and yielded quite low adsorptive removals of uranium.

4. Modelling of the dissolution kinetics

A kinetic study of the dissolution process was carried out based on the well-known shrinking core model and all three possible mechanisms as film diffusion control, surface reaction control and product layer diffusion control were studied [31] for possible fitting in the current work. The shrinking core model assumes that the reaction proceeds at



(a)



(b)

Fig. 10. Comparison of the control mechanisms governing the uranium recovery from (a) SiO₂M (b) f BHM.

the solid–liquid interface which moves into the solid core, that remains unreacted. Each of the controlling mechanism based model equation can be expressed as shown in Eqs (1–3):

$$x = k_F t \text{ for film diffusion control,} \quad (1)$$

$$1 - (1-x)^{1/3} = k_s t \text{ for surface reaction control} \quad (2)$$

$$1 + 2(1-x) - 3(1-x)^{2/3} = k_D t \text{ for product layer diffusion control} \quad (3)$$

Where x is the reacted fraction at time t and k_F , k_S , k_D are apparent rate constants expressed as in Eqs (4)–(6):

$$K_F = \frac{3bkC_{\text{HNO}_3}}{\rho} \quad (4)$$

$$k_S = \frac{bkMC_{\text{HNO}_3}}{\rho r_0} \quad (5)$$

$$k_D = \frac{2bMD_e C_{\text{HNO}_3}}{\rho r_0^2} \quad (6)$$

In Eqs (4)–(6), b is the stoichiometric coefficient; M is the molecular weight of reacted substance; ρ is the density of reacted particle; r_0 is the initial particle radius; k is the intrinsic rate constant; D_e is the effective diffusivity and C_{HNO_3} is the bulk concentration of HNO_3 .

Fig. 10 a & b shows the fitting results for shrinking core model for SiO_2M and ^fBHM , respectively. Comparing the figures, it can be seen that the product layer diffusion control model is the best fit with correlation coefficient as 0.973 and standard deviation 0.0084 rather than surface reaction control model (correlation coefficient 0.9693 and standard deviation 0.0119) or film diffusion model (correlation coefficient 0.9679 and standard deviation 0.023) for both adsorbents as SiO_2M and ^fBHM . The conclusion of best fitting model is based on the relative values of the obtained correlation coefficients (highest value) and standard deviation (lowest value) for the product layer diffusion control model.

The data was also used to determine the value of k_D according to Eq. (7) at different values of temperature, similar to our previous work [31]. The rate constant, k_D can be expressed as follows:

$$k_D = k_0 e^{-\frac{E_a}{RT}} \quad (7)$$

The linear form of Eq. (7) can be expressed as shown in Eq. (8):

$$\ln(k_D) = \ln(k_0) - \frac{E_a}{RT} \quad (8)$$

In Eq. (8), k_0 is the Arrhenius constant, E_a is the activation energy, T is the temperature and R is the universal gas constant [31]. The activation energy was calculated using the plots of rate constants at different temperatures using the linear form of Arrhenius equation. The summary of the results are given in Table 1. The activation energy in both cases is less than 20 kJ mol^{-1} (confirming the diffusion-controlled mechanism). Interestingly, the activation energy required to recover uranium from ^fBHM are almost comparable to SiO_2M .

5. Conclusions

The present work established the intensified recovery of uranium from the substrates. Based on the demonstrated results, it was observed that the process could be utilized widely in nuclear industries to recover the radioactive material uranium by intensified dissolution using ultrasound from functionalized and non-functionalized microparticles. It was observed that in 45 min, the uranium recovery was 34% for the SiO_2M and 39% for the ^fBHM . The intensification due to ultrasound was more pronounced (five times) in case of SiO_2M , than that (two times) in case of ^fBHM compared to the silent approach. The uranium metal recovered could be recycled in the nuclear fuel cycle, thereby preventing unnecessary waste of precious natural resources. The morphology of the

Table 1

Kinetics of uranium recovery from SiO_2M and ^fBHM .

S no.	Substrate	Activation Energy (kJ/mol)	Control mechanism
1	SiO_2M	17.8	Product layer diffusion control: $1 + 2(1-x) - 3(1-x)^{2/3} = \frac{-17842}{e^{-RT}} t$
2	^fBHM	19.6	Product layer diffusion control: $1 + 2(1-x) - 3(1-x)^{2/3} = \frac{-19596}{e^{-RT}} t$

substrates after the sonication was studied to understand the reusability aspect of the substrate. It was observed that structure of the SiO_2M remained unchanged after sonication, while the morphology of the ^fBHM gets deformed mainly due to the action of acid at higher concentration beyond 4 M acid concentration. This shows that while SiO_2M can be easily reused for adsorption of uranium in the second cycle (to remove around 69% of the initial concentration of the uranyl solution), such recycling of the substrate was possible with the biohybrid only if it is treated using acid at concentration less than 4 M. However, the loss of adsorption sites due to acid treatment lowered its adsorption capacity to 58% in the second cycle compared to 92% reported at the initial adsorption stage.

Recovery and reuse of both (the nuclear material and the sorbent) would ensure a low-waste nuclear remediation technique, thereby aligning with UN's Sustainable Development Goals (SDGs). The kinetics of the metal recovery from the substrates was determined and the dissolution of uranium from biohybrid showed slightly higher activation energy than the silica microparticles.

CRediT authorship contribution statement

S. Lahiri: Conceptualization, Methodology, Investigation, Writing - original draft. **A. Mishra:** Methodology, Resources, Investigation, Writing - original draft. **D. Mandal:** Supervision. **R.L. Bhardwaj:** Supervision, Writing - review & editing, Project administration. **P.R. Gogate:** Supervision, Writing - review & editing.

Declaration of Competing Interest

The authors declare that they have no known competing financial interests or personal relationships that could have appeared to influence the work reported in this paper.

Acknowledgments

The authors would like to thank V. K. Tapas and V. Mishra for the analytical instruments/ facilities as well as J. S. Melo, M. Mascarenhas and A. Sharma for their support and motivation towards this work. The work was funded by Bhabha Atomic Research Centre, India and we also acknowledge the funding support.

Data availability

The raw/processed data required to reproduce these findings cannot be shared at this time as the data also forms part of an ongoing study.

References

- [1] D.C. Shin, Y.S. Kim, H.S. Moon, J.Y. Park, International trends in risk management of groundwater radionuclides, *J. Environ. Toxicol.* 17 (2002) 273–284.

- [2] Y Cheng, X. Sun, X. Liao, B. Shi, 2011. Adsorptive recovery of uranium from nuclear fuel industrial wastewater by titanium loaded collagen fiber, *Chin. J. Chem. Eng.* 19 (4) (2011) 592–597.
- [3] X. Yi, Z. Xu, Y. Liu, X. Guo, M. Ou, X. Xu, Highly efficient removal of uranium (IV) from wastewater by polyacrylic acid hydrogels, *RSC Adv.* 11 (2017) (2017) 6278–6287.
- [4] K.T. Dreher, Removal of uranium and molybdenum from uranium mine wastewater, M Tech Thesis, New Mexico Institute of Mining and Technology (1980).
- [5] D. K. Singh, S. Mondal & J. K. Chakravarty (2016) Recovery of Uranium from Phosphoric Acid: A Review, Solvent Extraction and Ion Exchange, 34:3, 201–225, DOI: 10.1080/07366299.2016.1169142.
- [6] N. Haneklaus, A. Bayok, V. Fedchenko, Phosphate Rocks and Nuclear Proliferation, *Science & Global Security* 25 (3) (2017) 143–158, <https://doi.org/10.1080/08929882.2017.1394061>.
- [7] N. Haneklaus, Unconventional uranium resources from phosphates, in: E. Greenspan (ed.), *Encyclopedia of Nuclear Energy*, Elsevier, 2021, 286–291. <https://doi.org/10.1016/B978-0-12-819725-7.00152-5>.
- [8] K. Dungan, G. Butler, F.R. Livens, L.M. Warren, Uranium from seawater – Infinite resource or improbable aspiration? *Prog. Nucl. Energy* 99 (2017) 81–85.
- [9] N. Haneklaus, Y. Sun, R. Bol, B. Lottermoser, E. Schnug, To Extract, or not to Extract Uranium from Phosphate Rock, that is the Question, *Environ. Sci. Technol.* 51 (2) (2016) 753–754, <https://doi.org/10.1021/acs.est.6b05506>.
- [10] W.A. Abbasi, M. Streat, Adsorption of uranium from aqueous solutions using activated carbon, *Sep. Sci. Technol.* 29 (1994) (1994) 1217–1230.
- [11] R. Qadeer, J. Hanif, Kinetics of uranium (VI) ions adsorption on activated charcoal from aqueous solutions, *Radiochim. Acta.* 65 (1994) 259–263.
- [12] S. Xie, C. Zhang, X. Zhou, J. Yang, X. Zhang, J. Wang, Removal of uranium (VI) from aqueous solution by adsorption of hematite, *J. Environ. Radioact.* 100 (2009) 162–166.
- [13] M. Konstantinou, A. Demetriou, I. Pashalidis, Adsorption of hexavalent uranium on undunite, *Global NEST J.* 9 (2007) 229–236.
- [14] I. Sierra, D. Perez-Quintanilla, Heavy metal complexation on hybrid mesoporous silicas: an approach to analytical applications, *Chem. Soc. Rev.* 42 (2013) 3792–3807.
- [15] S. Chen, J. Hong, H. Yang, J. Yang, Adsorption of uranium (VI) from aqueous solution using a novel graphene oxide activated carbon felt composite, *Environ. Radioact.* 126 (2013) 253–258.
- [16] M. Hua, S. Zhang, B. Pan, W. Zhang, L. Lv, Q. Zhang, Heavy metal removal from water/wastewater by nanosized metal oxides: a review, *J. Hazard. Mater.* 211–212 (2012) 317–331.
- [17] M. Ahmedna, W.E. Marshall, A.A. Husseiny, R.M. Rao, I. Goktepe, The use of nutshell carbons in drinking water filters for removal of trace metals, *Water Res.* 38 (2004) 1062–1068.
- [18] A.F. Ngomsik, A. Bee, M. Draye, G. Cote, V. Cabuil, Magnetic nano- and microparticles for metal removal and environmental applications: a review, *C. R. Chim.* 8 (2005) 963–970.
- [19] M. Hiraide, J. Iwasawa, S. Hiramatsu, H. Kawaguchi, Use of surfactant aggregates form on alumina for the preparation of chelating sorbents, *Anal. Sci.* 11 (1995) 611–615.
- [20] J. Li, Y. Shi, Y. Cai, S. Moua, G. Jiang, Adsorption of di-ethylphthalate from aqueous solutions with surfactant-coated nano/microsized alumina, *Chem. Eng. J.* 140 (2008) 214–220.
- [21] A. Mishra, J. Kumar, J.S. Melo, An optical microplate biosensor for the detection of methyl parathion pesticide using a bio-hybrid of *Sphingomonas sp.* cells-silica nanoparticles, *Biosens. Bioelectron.* 87 (2017) 332–338.
- [22] A. Mishra, J. Kumar, J.S. Melo, Silica based bio-hybrid materials and their relevance to bionanotechnology, *Austin J Plant Biol.* 6 (1) (2020) 1024.
- [23] A. Mishra, J.S. Melo, A. Agrawal, Y. Kashyap, D. Sen, Preparation and application of silica nanoparticles-*Ocimum basilicum* seeds bio-hybrid for the efficient immobilization of invertase enzyme, *Colloids and Surfaces B* 188 (2020), 110796.
- [24] P. Michard, E. Guibal, T. Vincent, P.L. Cloirec, Sorption and desorption of uranyl ions by silica gel: pH, particle size and porosity effects, *Microporous Mater.* 5 (1996) 309–324.
- [25] T. Reich, H. Moll, T. Arnold, M.A. Denecke, C. Hennig, G. Geipel, G. Bernhard, H. Nitsche, P.G. Allen, J.J. Bucher, N.M. Edelstein, D.K. Shuh, An EXAFS study of uranium (IV) sorption onto silica gel and ferrihydrite, *J. Electron Spectrosc. Relat. Phenom.* 96 (1998) 237–243.
- [26] U. Gabriel, L. Charlet, C.W. Schlappfer, J.C. Vial, A. Brachmann, G. Geipel, Uranyl Surface Speciation on Silica Particles Studied by Time-Resolved Laser-Induced Fluorescence Spectroscopy, *J. Colloid Interface Sci.* 239 (2001) 358–368.
- [27] H.I. Lee, J.H. Kim, J.M. Kim, S. Kim, J.N. Park, J.S. Hwang, J.W. Yeon, Y. Jung, Application of ordered nanoporous silica for removal of uranium ions from aqueous solution, *J. Nanosci. Nanotechnol.* 10 (2010) 217–221.
- [28] P. Metilda, J.M. Gladis, T.P. Rao, Catechol functionalized aminopropyl silica gel: synthesis, characterization and preconcentrative separation of uranium (VI) from thorium (IV), *Radiochim. Acta* 93 (2005) 219–224.
- [29] P.G. Krishna, J.M. Gladis, K.S. Rao, T.P. Rao, G.R.K. Naidu, Synthesis of xanthate functionalized silica gel and its application for the preconcentration and separation of uranium(VI) from inorganic components, *J. Radioanal. Nucl. Chem* 266 (2005) 251–257.
- [30] A. Mishra, J.S. Melo, D. Sen, S.F. D' Souza, Evaporation induced self assembled microstructures of silica nanoparticles and *Streptococcus lactis* cells as sorbent for uranium (VI), *J. Colloid. Interf. Sci.* 414 (2014) 33–40.
- [31] C. Kütahyalı, M. Eral, Selective adsorption of uranium from aqueous solutions using activated carbon prepared from charcoal by chemical activation, *Sep. Purif.* 40 (2004) 109–114.
- [32] S. Lahiri, D. Mandal, R.L. Bhardwaj, P.R. Gogate, Intensified dissolution of uranium from graphite substrate using ultrasound, *Ultrason. Sonochem.* 65 (2020), 105066.
- [33] S.A. Elder, Cavitation Microstreaming, *J. Acoust. Soc. Am.* 31 (1959) 54.
- [34] K.S. Suslick, Sonochemistry, *Science* 247 (1990) 1439–1445.
- [35] B. Pesic, T. Zhou, Application of ultrasound in extractive metallurgy: sonochemical extraction of nickel, *Metall. Trans.* 23B (1992) 13–22.
- [36] M.E. Entezari, P. Kruus, The effect of frequency on sonochemical reactions II: Temperature and Intensity effects, *Ultrason. Sonochem.* 3 (1996) 19–24.
- [37] M.E. Entezari, P. Kruus, The effect of frequency on sonochemical reactions I: absolute rates, *Ultrason. Sonochem.* 1 (1994) S75–S79.
- [38] K.L. Narayana, K.M. Swamy, K.S. Rao, J.S. Murthy, Leaching of metals from ores with ultrasound, *Min. Pro. Ext. Met. Rev.* 16 (1997) 239–259.
- [39] S. Lahiri, D. Mandal, P.R. Gogate, A. Ghosh, R.L. Bhardwaj, Cavitation-assisted decontamination of yttria from graphite of different densities, *Ultrason. Sonochem.* 73 (2021), 105520.
- [40] F. Fan, Z. Qin, J. Bai, W.D. Rong, F. Fan, W. Tian, X. Wu, Y. Wang, L. Zhao, Rapid removal of uranium from aqueous solutions using magnetic Fe₃O₄@SiO₂ composite particles, *J. Environ. Radioact.* 106 (2012) 40–46.
- [41] A. Lopez-Malo, S. Guerrero, S.M. Alzamora, Saccharomyces cerevisiae thermal inactivation kinetics combined with ultrasound, *J. Food Protect.* 62 (10) (1999) 1215–1217.
- [42] S.A. Cochran, M.R. Prausnitz, Sonoluminescence as an Indicator of Cell Membrane Disruption by Acoustic Cavitation, *Ultrasound in Med & Biol* 27 (6) (2001) 841–850.
- [43] P. Belgrader, D. Hansford, G.T. Kovacs, K. Venkateswaran, R.J. Mariella, F. Milanovich, S. Nasarabadi, M. Okuzumi, F. Pourahmadi, M.A. Northrup, A minisonicator to rapidly disrupt bacterial spores for DNA analysis, *Anal. Chem.* 71 (19) (1999) 4232–4236.
- [44] H.R. Guzman, D.X. Nguyen, S. Kahn, M.R. Prausnitz, Ultrasound-mediated disruption of cell membranes. I. Quantification of molecular uptake and cell viability, *J Acoust Soc Am* 110 (1) (2001) 588–596.
- [45] A.E. Egger, C. Rappel, M.A. Jakupcic, C.G. Hartinger, P. Heffeter, B.K. Keppler, Development of an experimental protocol for uptake studies of metal compounds in adherent tumor cells, *J. Anal At Spectrom.* 24 (1) (2009) 51–61.
- [46] M.P. Murphy, Nitric oxide and cell death, *Biochimica et Biophysica Acta* 1411 (2–3) (1999) 401–414.
- [47] L.M. Loth, G.M. Begun, Raman spectra of uranyl ion and its hydrolysis products in aqueous HNO₃, *J. Phys. Chem.* 85 (1981) 549–556.